Identifying and Mitigating Charge Instabilities in Shallow Diamond Nitrogen-Vacancy Centers

Dolev Bluvstein, Zhiran Zhang, and Ania C. Bleszynski Jayich
Department of Physics, University of California, Santa Barbara, California 93106, USA

(Received 3 October 2018; published 19 February 2019)

The charge degree of freedom in solid-state defects fundamentally underpins the electronic spin degree of freedom, a workhorse of quantum technologies. Here we measure, analyze, and control charge-state behavior in individual near-surface nitrogen-vacancy (NV) centers in diamond, where NV^- hosts the metrologically relevant electron spin. We find that NV^- initialization fidelity varies between individual centers and over time; we alleviate the deleterious effects of reduced NV^- initialization fidelity via logic-based initialization. Importantly, we also show that NV^- can ionize in the dark on experimentally relevant timescales, and we introduce measurement protocols that mitigate the compromising effects of charge conversion on spin measurements. We identify tunneling to a single local electron trap as the mechanism for ionization in the dark, and we develop novel NV-assisted techniques to control and read out the trap charge state. Our understanding and command of the NV's local electrostatic environment will simultaneously guide materials design and provide unique functionalities with NV centers.

DOI: 10.1103/PhysRevLett.122.076101

Solid-state defects are important tools in quantum technologies. Prominent examples include nitrogen-vacancy [1–4] and silicon-vacancy [5,6] centers in diamond, defects in silicon carbide [7–9], and donors in silicon [10–12], where the electronic spin degree of freedom is commonly employed for quantum tasks such as sensing or computing. Importantly, these defects also harbor a charge degree of freedom. The charge degree of freedom sets the number of unpaired electrons that constitute the spin degree of freedom, and so control over spin necessitates control over charge. Lack of charge control can lead to deleterious effects on the defect's functionality as a qubit or sensor. However, with sufficient understanding and control, the charge degree of freedom can be harnessed for a variety of applications such as high fidelity spin readout [13–16], super-resolution microscopy [17–19], enhancing quantum coherence [5,20], and electrical sensing modalities [21,22].

Shallow, negatively charged nitrogen-vacancy (NV^-) centers in diamond have received particular attention for their sensing abilities, recently demonstrating nanoscale magnetic imaging of condensed matter [23,24] and biological systems [25–27], thermal imaging [28,29], and electrical conductivity imaging [30]. Shallow NV^- centers can also interface with other quantum elements in hybrid quantum systems [31–33]. On the other hand, neutral NV^0 centers have not achieved promising electron spin control but are commonly observed [34–36] and result in undesired background in NV^- experiments. Notably, the diamond surface is observed to preferentially convert NV^- to NV^0 [37–39], thus imposing a clear obstacle to nanoscale sensing applications, where the NV depth is critical to both sensitivity and spatial resolution [40,41].

Under optical illumination in bulk diamond, single NV centers continuously interconvert between negative and neutral charge states as the NV exchanges electrons with the electronic bands, where the steady-state NV^- population reaches ≈ 0.75 under commonly used cw 532-nm excitation [13,15,42–45]. For near-surface NV centers, however, understanding of photoinduced charge interconversion is largely limited to ensemble measurements, which explain surface-induced NV^- ionization as a result of upwards band bending from surface acceptor states [37,46]. In the absence of optical illumination, recent studies on NV ensembles have shown that NV charge states can be both unstable in time [47–49] and stable on timescales exceeding weeks [50–52]. Instability of shallow NV^- centers under illumination or in the dark can directly compromise computing and sensing modalities, yet understanding is still limited.

In this Letter, we discover several intriguing charge-state behaviors in single shallow NV centers, both under illumination and in the dark; we focus, in particular, on the experimentally relevant implications for sensing and identifying the microscopic origins of charge-state instability. We find that the fidelity of optical initialization into NV^- exhibits large variations between shallow NV centers as well as over time. We identify reduced NV^- initialization fidelity as the primary cause of reduced spin measurement contrast in shallow NVs, which we alleviate by implementing logic-based charge initialization. We also find that

shallow NV^- centers can ionize to NV^0 in the dark, which we methodically identify as tunneling to a single local electron trap. We achieve control and readout of the trap charge state and measure its optical ionization properties. Further, we show that charge conversion in the dark can produce anomalous signatures in spin measurements and, at worst, will appear indistinguishable from T_1 and T_2 spin decay; we relieve this detrimental effect by measurement protocols we present here.

The experimental setup consists of a home-built, room-temperature confocal microscope for optically addressing NV^- and NV^0 centers, which have zero-phonon lines at 637 and 575 nm, respectively [35]. We use a 532-nm laser for initialization and NV^- spin state readout, and we use a 594-nm laser for charge-state readout. Under 594-nm excitation, NV^- is $\sim 40\times$ brighter than NV^0 in our setup. NV centers are formed by ^{14}N ion implantation at 4 keV with a dosage of 5.2×10^{10} ions/cm^2 into a 150-μm-thick Element Six electronic grade (100) diamond substrate, followed by subsequent annealing at 850 °C for 2.5 h (see Supplemental Material Note 1 [53] for further details). In this Letter, we present data for several individual NV centers, denoted NV1, NV2, etc. The NV centers' depths are experimentally measured via proton NMR [57,58] and range between ~3 and 17 nm (see Supplemental Material Fig. S5 [53]).

We first report on NV^- initialization fidelity ρ^- and its variation in near-surface NV centers. ρ^- is defined as the probability to be in NV^- immediately after 532-nm illumination. ρ^- is an important parameter because it directly affects NV^- measurement sensitivity; the NV^0 state gives unwanted background while not contributing to the sensing signal. Here we find that ρ^- varies strongly for shallow NV centers and can be significantly less than 0.75, the commonly reported value for bulk NV centers [13,15,42–45]. In Figs. 1(c) and 1(d), we measure the NV^- initialization fidelity ρ^- for two near-surface NVs in the same sample. Plotted are the statistics for the number of photons measured during a 1-ms-long 594-nm readout pulse following a 532-nm initialization pulse. The photon statistics are fit to the model in Supplemental Material Note 2.1 [53], which is approximately the sum of two Poisson distributions for NV^- and NV^0 [13,59]. The relative contribution of the NV^- distribution yields ρ^-. For NV1 presented in Fig. 1(c), we extract $\rho^- = 0.78(1)$, reproducing the typical reported value for single NVs in bulk diamond. In contrast, we measure $\rho^- = 0.05(1)$ for NV2, shown in Fig. 1(d). From a sample of 67 individual centers, we measure an average $\langle \rho^- \rangle = 0.59$ and a standard deviation $\sigma_{\rho^-} = 0.15$ (see Supplemental Material Fig. S1 [53]).

We also find that ρ^- can vary in time for the same NV center, on timescales spanning seconds to months. To capture the faster dynamics, in Fig. 1(e) we plot two datasets, each consisting of 1000 consecutive 1-ms-long

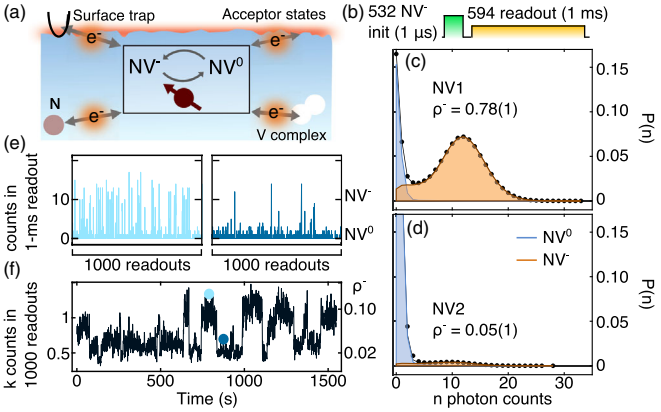

FIG. 1. NV charge-state characteristics vary with different local charge environments. (a) The charge state of proximal nitrogen (N) centers, vacancy (V) complexes, surface electron traps, and surface acceptor states can all affect the NV charge state. (b) Pulse sequence to measure NV^- initialization fidelity ρ^- under 532-nm illumination. ρ^- is the probability to be in NV^- immediately after the 532-nm pulse. (c),(d) Probability of measuring n photons $P(n)$ for charge stable (c) and charge unstable (d) NV centers in the same sample. Black curve is the sum of the fitted NV^- and NV^0 distributions. (e) Two sets of 1000 consecutive 1-ms-long measurements from the same data comprising the distribution in (d). (f) Consecutive measurements binned into sets of 1000 (1 s each).

readouts on NV2. The two datasets, taken 2 s apart, show a notable difference in the probability of initializing into NV^-, as measured by photon counts, indicating that ρ^- is larger in the first dataset than in the second. Coarse graining the data by binning 1000 consecutive measurements yields the data in Fig. 1(f), which shows that ρ^- takes on discrete values that are stable on timescales of seconds to minutes. This discrete behavior suggests that the NV charge state is governed by discrete metastable configurations of the local charge environment. In practice, this environment-induced slow blinking, which is also observed under cw 532-nm excitation and is distinct from photoinduced hopping between NV charge states, can reduce the sensitivity of near-surface NV centers by introducing substantial slow noise into measurements.

Our measurements also reveal that the average ρ^- decreases on timescales of days to months, and we find that this decrease is strongly correlated to environmental changes at the diamond surface. As a practical metric for ρ^-, we monitor the NV^- spin fluorescence contrast in a Rabi oscillation measurement; the contrast is reduced when the NV spends more time in the neutral NV^0 state, which contributes spin-independent background fluorescence. Figure 2(a) plots the Rabi contrast of NV1 as a function of time after a standard surface preparation protocol consisting of acid cleaning and oxygen annealing (see Supplemental Material Note 1 [53]). The Rabi contrast was stable at 35% for 130 days before suddenly decreasing to 5% over a span of 20 days. Other NV centers exhibit similar

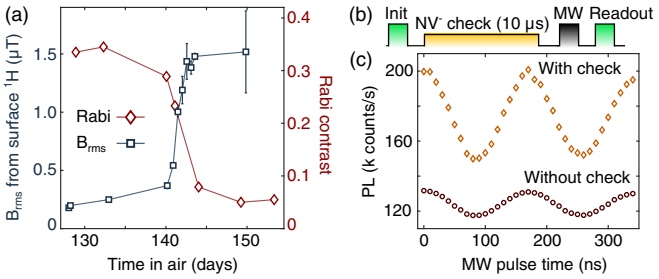

FIG. 2. (a) Rabi contrast and root-mean-square magnetic field B_{rms} produced by surface ^{1}H versus time under ambient conditions. Rabi contrast is defined as the peak-to-peak amplitude of the photoluminescence (PL) oscillations divided by the maximum PL. (b) Rabi pulse sequence for (c) including logic-based charge initialization protocol. (c) Photoluminescence-based measurement of Rabi oscillations on charge unstable NV center ($\rho^- \approx 0.15$), with (orange diamonds) and without (red circles) using precheck protocol.

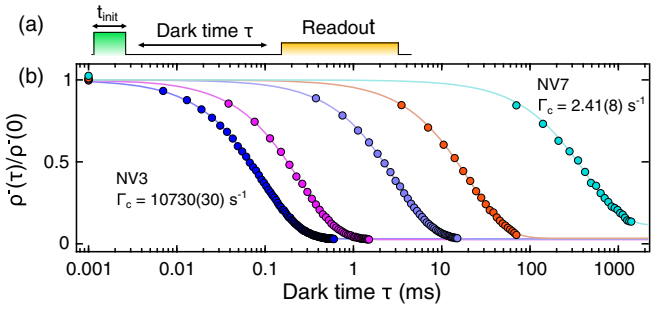

FIG. 3. NV^- survival probability in the dark after 532-nm initialization. (a) Measurement sequence for (b). (b) NV^- ionization in the dark measured on five representative NV centers; solid curves are fits to the exponential decay in Eq. (1). Left to right, $\Gamma_c = 10730(30)$, 4030(10), 331(1), 48.9(6), 2.41(8) s^{-1}.

behavior, with, e.g., NV2 exhibiting a drop in ρ^- from $\approx$0.75 to 0.05 over several months. Notably, cleaning the surface induces a partial or full recovery of ρ^-, suggesting that changes in ρ^- are dominated by surface effects.

Critically, as shown in Fig. 2(a), we find that the reduction in Rabi contrast on NV1 (measured depth $\sim$3.5 nm) is strongly correlated with an increase in the number of ^{1}H nuclear spins on the diamond surface, as measured via NV-based nuclear magnetic resonance [26,60]. The root-mean-square magnetic field B_{rms} produced by surface ^{1}H is measured with an XY8-k sensing sequence (see Supplemental Material Fig. S5 [53]) [57,61]. The reason for the increased ^{1}H is unclear, but we make a few observations. The 1.5 μT B_{rms} value measured after long air exposure is too large to be exclusively due to a two-dimensional surface hydrogen termination layer, indicating that other adsorbates such as water or hydrocarbons are contributing. Further, other NV centers did not exhibit similar changes in contrast and ^{1}H density between days 130 and 150, and hence we speculate that laser illumination plays a role, as we illuminated only NV1 during that period. Maintaining high Rabi contrast over extended periods of time is critical for NV-based sensing, and the correlation discovered here motivates further investigation.

The deleterious effects of low ρ^- on Rabi contrast can be alleviated by implementing a measurement protocol [Fig. 2(b)] that checks for successful NV^- initialization prior to the spin measurement sequence. In Fig. 2(c), we plot a Rabi measurement with and without this precheck; the spin measurement contrast increases from 14 to 50 k counts/s and the measured signal-to-noise ratio increases threefold. This result also confirms that poor NV^- initialization fidelity is the dominant source of reduced Rabi contrast. In demonstrating this precheck technique in Fig. 2(b), we postselect on the raw data by removing measurements where no photons are detected during the 10-μs, 594-nm NV^- check in Fig. 2(b). In practice, to increase measurement sensitivity, one would integrate on-the-fly logic to reinitialize after a failed precheck.

We now turn to a discussion of NV charge-state dynamics in the dark. In Fig. 3(b), we plot the NV^- population as a function of dark wait time after a 532-nm initialization pulse [Fig. 3(a)] for five NVs; we find NV^- ionizes to NV^0 in the dark with a wide distribution of decay times. All NVs fit well to a model of exponential decay

$$\rho^-(t)/\rho^-(0) = 1 - A(1 - e^{-\Gamma_c t}), \tag{1}$$

where decay rate Γ_c, starting NV^- population $\rho^-(0)$, and decay amplitude A are free fit parameters. The five NVs plotted in Fig. 3 span 4 orders of magnitude in Γ_c, with timescales ranging from 100 μs to seconds. From a sample of 108 individual centers, approximately 10% of NVs have $\Gamma_c > 50$ s^{-1}, 10% have 50 $s^{-1} > \Gamma_c > 20$ s^{-1}, 30% have 20 $s^{-1} > \Gamma_c > 1$ s^{-1}, and 50% have $\Gamma_c < 1$ s^{-1}. We do not observe a dependence of Γ_c on magnetic field or a strong correlation with NV depth (see Supplemental Material Table S1 [53]). See Supplemental Material Note 2.2 [53] for details of measuring $\rho^-(t)$.

We find the dark ionization process is highly dependent on initialization power and duration. Figure 4(a) plots the charge decay observed on NV5 [middle curve in Fig. 3(b)] for initialization times $t_{\mathrm{init}} = 3$ and 200 μs. Interestingly, the two fits yield the same Γ_c but A changes substantially; as $t \to \infty$, NV^- decays to NV^0 in 98% of the measurement shots for $t_{\mathrm{init}} = 200$ μs, but only in 42% of the shots with $t_{\mathrm{init}} = 3$ μs. To arrive at a more quantitative understanding, we repeat the measurement in Fig. 4(a), varying t_{init} over a large range of values. The dependence of A on t_{init} is plotted in Fig. 4(b) at six laser powers, and the result is fit well by an exponential with a rate that increases with power. Γ_c does not change with t_{init} or power (see Supplemental Material Fig. S2 [53]). We note that, in Fig. 3, the laser

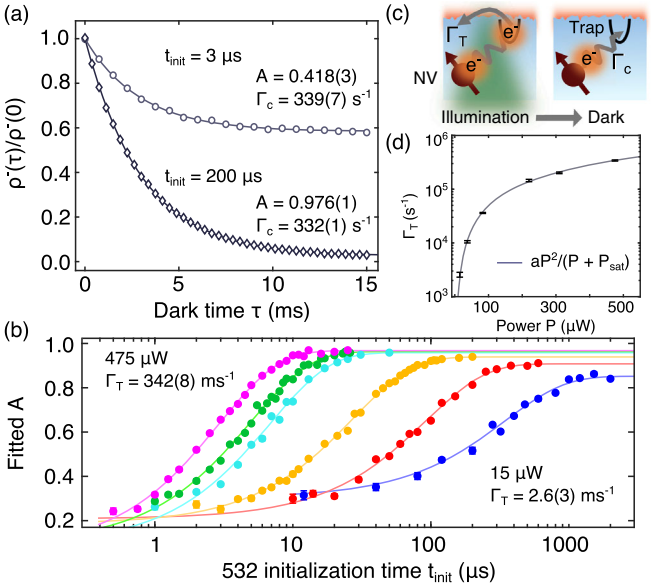

FIG. 4. (a) Charge decay measurement [Fig. 3(a)] on NV5 with 225-μW, 532-nm excitation for $t_{\mathrm{init}} = 3$ μs (light circles) and 200 μs (dark diamonds). Solid curves are fits to Eq. (1). (b) Fitted values of A for varied initialization times at six laser powers ranging from 15 to 475 μW. The solid curves are fits to a model of exponential saturation with rate $\Gamma_T + \Gamma_c$. (c) Model for charge decay: a local electron trap is ionized during initialization at rate Γ_T and captures an electron from NV^- at fixed tunneling rate Γ_c. A is then the probability that the trap is empty. (d) Trap ionization rate Γ_T versus laser power. Solid curve is a fit to $aP^2/(P + P_{\mathrm{sat}})$.

power and t_{init} were chosen on each NV such that A reaches its saturation value.

To explain the observations of Figs. 4(a) and 4(b), in Fig. 4(c) we present a model of electron tunneling to a single local electron trap with fixed tunneling rate Γ_c. If the trap is empty, NV^- will decay to NV^0 as $t \to \infty$; A then represents the probability that the trap is empty. In our model, the green illumination ionizes the trap at rate Γ_T and thus empties the trap with probability $A \sim 1 - \exp(-\Gamma_T t_{\mathrm{init}})$, as observed in Fig. 4(b). To repump the trap between measurement repetitions, we optically initialize into NV^- and wait in the dark for a time $> 3/\Gamma_c$. A key result is that the presence of multiple dominant traps is inconsistent with the data in Fig. 4. Multiple dominant traps would result in a non-monoexponential decay and necessitates that the fitted Γ_c increase with A, which we do not observe (see Supplemental Material Note 3 [53]). We find no dependence of Γ_c on A for all centers where Γ_c versus A is measured (NV3, NV4, NV5). With this analysis, we identify the mechanism for charge decay as tunneling to a single local electron trap. Moreover, we can quantitatively set the trap charge-state population by varying t_{init} as in Fig. 4(b).

We probe the ionization properties of the trap with our NV-assisted control and readout capabilities: we intentionally populate the trap via tunneling from NV^- to trap, then ionize the trap optically while repopulating NV^-, and finally measure the trap charge state via NV^- ionization in the dark. In Fig. 4(d), we plot the trap ionization rate Γ_T versus 532-nm laser power. We find Γ_T is fit well by a saturation model of $aP^2/(P + P_{\mathrm{sat}})$, where $a = 814(43)$ $\mathrm{s}^{-1}/\mu\mathrm{W}$, P is laser power, and the saturation power $P_{\mathrm{sat}} = 65(23)$ μW. This power dependence is consistent with trap ionization by a two-photon transition through an orbital excited state; we note that NV^- requires the energy of two 532-nm photons to photoionize [42], and we expect the trap is lower in energy than NV^-. In Fig. 4(b), we also observe that $A(t_{\mathrm{init}} = \infty)$ increases with laser power, which is qualitatively reproduced by $\Gamma_T/(\Gamma_T + \Gamma_c)$ as a consequence of the rate equations under illumination (see Supplemental Material Fig. S6 [53]). Physical trap candidates where tunneling could be energetically favorable include vacancy-related complexes, specifically divacancy [50,62] and surface sp^2 defects [63]. The lack of strong correlation between Γ_c and NV depth (Supplemental Material Table S1 [53]) is consistent with our observation of a single dominant trap and further suggests that the traps reside inside the diamond and/or that the traps are on the surface with a low density.

We now turn to a discussion of the detrimental effects of charge conversion in the dark on spin measurements, as well as the appropriate mitigation protocols. In Fig. 5(a), an exponential fit to a typical T_1 measurement on NV5 yields different relaxation rates depending on the duration of the green initialization pulse, indicating the presence of confounding effects that mask the true value of the spin T_1. The T_1 measurement in Fig. 5(a) employs a common-mode rejection technique referred to as a differential measurement: plotted is the difference between two PL measurements, one with and one without a microwave $|m_s = 0 \to 1\rangle$ π pulse immediately before readout [64]. The differential measurement alleviates effects of recombination in the dark, but

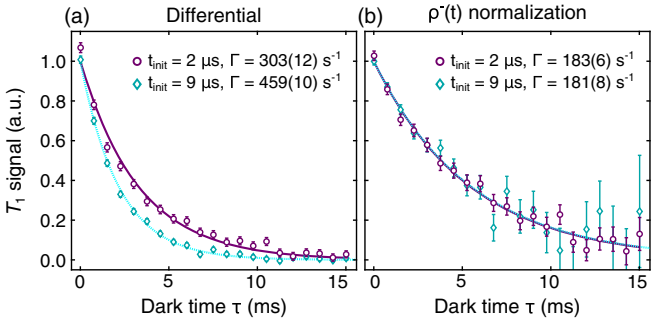

FIG. 5. Removing the effect of NV^- ionization in the dark from spin measurements. (a) Differential T_1 measurement on NV5, measured with a spin-to-charge sequence [13,30]. Initialization times of 2 μs (purple circles) and 9 μs (blue diamonds) yield inconsistent signals. Curves are fits to $\exp(-\Gamma t)$. (b) Normalizing for charge decay during the dark τ time for the signals in (a) renders agreement between the two measurements and yields Γ consistent with spin relaxation rates of other NVs in the same sample ($\Gamma_1 \sim 200 \pm 30$ s^{-1}).

importantly does not alleviate ionization in the dark (see Supplemental Material Note 4 [53]). A differential T_1 measurement in the case of ionization in the dark, as in Fig. 5(a), yields data $\mathrm{PL}_{\mathrm{diff},T_1}$ with

$$\mathrm{PL}_{\mathrm{diff},T_1}(t) = C\exp(-\Gamma_1 t)[\rho^-(t)/\rho^-(0)], \qquad (2)$$

where $\Gamma_1 \equiv 1/T_1$ and C describes the contrast between the spin states. For NV5 presented in Fig. 5, $t_{\mathrm{init}} = 2$ and 9 μs produce different $\rho^-(t)$ (Fig. 4), and thus fitting to $\exp(-\Gamma t)$ results in different values of Γ, neither of which are Γ_1. In practice, the biexponential decay of $\mathrm{PL}_{\mathrm{diff},T_1}$ may be indistinguishable from a monoexponential decay with $\Gamma \approx \Gamma_1 + A\Gamma_c$, and so we emphasize that NV^- ionization in the dark requires attention.

To fully mitigate charge ionization in the dark, in Fig. 5(b) we divide the data $\mathrm{PL}_{\mathrm{diff},T_1}$ by $\rho^-(t)$, which is measured separately in the same measurement sequence. In this way, we isolate the spin relaxation signal $\exp(-\Gamma_1 t)$, bringing the data and the fitted values of Γ into agreement for the two initialization times. The same analysis and mitigation protocol hold for T_2 measurements as well. See Supplemental Material Note 4 [53] for a discussion of other cases.

In conclusion, we show that the charge-state properties of NV centers both under illumination and in the dark depend on the charge configuration of the local discrete environment, and shallow NV centers can exhibit a significantly lower and less stable NV^- population relative to bulk NVs. These observations have direct implications in measurement sensitivity and validity, which can be addressed with the various measurement protocols we present here. Our results on environment-induced effects further indicate that, while bulk NV^- centers are reported to have superior stability, NV^- could become unstable due to, e.g., lattice damage from implantation or fabrication: our analysis and protocols are then directly applicable in these possible situations. We also develop techniques to control and read out the charge state of local electron traps, which future experiments could use to directly identify the trap's structure and characterize the NV-trap tunneling mechanism [65]. For instance, one can measure NV-trap separation by measuring trap-state-dependent electric fields [66,67], or one could measure the trap position in the band gap by varying the optical excitation energy. On the other hand, the NV-trap tunneling mechanism could be utilized for quantitative and highly sensitive measurements of electrochemical potentials or for the production of tunable local electric and magnetic fields.

We thank Claire McLellan, Amila Ariyaratne, Nathalie de Leon, Norman Yao, Patrice Bertet, and Chris Van de Walle for helpful discussions. We acknowledge partial support by a PECASE award from the Air Force Office of Scientific Research and partial support from NSF CAREER Grant No. DMR-1352660. D. B. acknowledges funding from the Microscopy Society of America and the Barry Goldwater Foundation.

[1] M. W. Doherty, N. B. Manson, P. Delaney, F. Jelezko, J. Wrachtrup, and L. C. Hollenberg, Phys. Rep. **528**, 1 (2013).
[2] L. Childress, M. V. Gurudev Dutt, J. M. Taylor, A. S. Zibrov, F. Jelezko, J. Wrachtrup, P. R. Hemmer, and M. D. Lukin, Science **314**, 281 (2006).
[3] F. Jelezko, T. Gaebel, I. Popa, A. Gruber, and J. Wrachtrup, Phys. Rev. Lett. **92**, 076401 (2004).
[4] A. Gruber, A. Dräbenstedt, C. Tietz, L. Fleury, J. Wrachtrup, and C. von Borczyskowski, Science **276**, 2012 (1997).
[5] B. C. Rose, D. Huang, Z.-H. Zhang, P. Stevenson, A. M. Tyryshkin, S. Sangtawesin, S. Srinivasan, L. Loudin, M. L. Markham, A. M. Edmonds, D. J. Twitchen, S. A. Lyon, and N. P. de Leon, Science **361**, 60 (2018).
[6] T. Müller, C. Hepp, B. Pingault, E. Neu, S. Gsell, M. Schreck, H. Sternschulte, D. Steinmüller-Nethl, C. Becher, and M. Atatüre, Nat. Commun. **5**, 3328 (2014).
[7] D. J. Christle, A. L. Falk, P. Andrich, P. V. Klimov, J. U. Hassan, N. Son, E. Janzén, T. Ohshima, and D. D. Awschalom, Nat. Mater. **14**, 160 (2015).
[8] W. F. Koehl, B. B. Buckley, F. J. Heremans, G. Calusine, and D. D. Awschalom, Nature (London) **479**, 84 (2011).
[9] M. Widmann, S.-Y. Lee, T. Rendler, N. T. Son, H. Fedder, S. Paik, L.-P. Yang, N. Zhao, S. Yang, I. Booker, A. Denisenko, M. Jamali, S. A. Momenzadeh, I. Gerhardt, T. Ohshima, A. Gali, E. Janzén, and J. Wrachtrup, Nat. Mater. **14**, 164 (2015).
[10] A. M. Tyryshkin, S. Tojo, J. J. L. Morton, H. Riemann, N. V. Abrosimov, P. Becker, H.-J. Pohl, T. Schenkel, M. L. W. Thewalt, K. M. Itoh, and S. A. Lyon, Nat. Mater. **11**, 143 (2012).
[11] F. A. Zwanenburg, A. S. Dzurak, A. Morello, M. Y. Simmons, L. C. L. Hollenberg, G. Klimeck, S. Rogge, S. N. Coppersmith, and M. A. Eriksson, Rev. Mod. Phys. **85**, 961 (2013).
[12] A. Morello, J. J. Pla, F. A. Zwanenburg, K. W. Chan, K. Y. Tan, H. Huebl, M. Möttönen, C. D. Nugroho, C. Yang, J. A. van Donkelaar, A. D. C. Alves, D. N. Jamieson, C. C. Escott, L. C. L. Hollenberg, R. G. Clark, and A. S. Dzurak, Nature (London) **467**, 687 (2010).
[13] B. J. Shields, Q. P. Unterreithmeier, N. P. de Leon, H. Park, and M. D. Lukin, Phys. Rev. Lett. **114**, 136402 (2015).
[14] G. Wolfowicz, C. P. Anderson, A. L. Yeats, S. J. Whiteley, J. Niklas, O. G. Poluektov, F. J. Heremans, and D. D. Awschalom, Nat. Commun. **8**, 1876 (2017).
[15] D. A. Hopper, R. R. Grote, A. L. Exarhos, and L. C. Bassett, Phys. Rev. B **94**, 241201 (2016).
[16] P. Siyushev, H. Pinto, M. Vörös, A. Gali, F. Jelezko, and J. Wrachtrup, Phys. Rev. Lett. **110**, 167402 (2013).
[17] M. Gu, Y. Cao, S. Castelletto, B. Kouskousis, and X. Li, Opt. Express **21**, 17639 (2013).
[18] E. Bersin, M. Walsh, S. Mouradian, M. Trusheim, T. Schröder, and D. Englund, arXiV:1805.06884.
[19] X. Chen, C. Zou, Z. Gong, C. Dong, G. Guo, and F. Sun, Light Sci. Appl. **4**, e230 (2015).

[20] M. Pfender, N. Aslam, P. Simon, D. Antonov, G. Thiering, S. Burk, F. Fávaro de Oliveira, A. Denisenko, H. Fedder, J. Meijer, J. A. Garrido, A. Gali, T. Teraji, J. Isoya, M. W. Doherty, A. Alkauskas, A. Gallo, A. Grüneis, P. Neumann, and J. Wrachtrup, Nano Lett. **17**, 5931 (2017).
[21] S. Karaveli, O. Gaathon, A. Wolcott, R. Sakakibara, O. A. Shemesh, D. S. Peterka, E. S. Boyden, J. S. Owen, R. Yuste, and D. Englund, Proc. Natl. Acad. Sci. U.S.A. **113**, 3938 (2016).
[22] G. Wolfowicz, S. J. Whiteley, and D. D. Awschalom, Proc. Natl. Acad. Sci. U.S.A. **115**, 7879 (2018).
[23] L. Thiel, D. Rohner, M. Ganzhorn, P. Appel, E. Neu, B. Müller, R. Kleiner, D. Koelle, and P. Maletinsky, Nat. Nanotechnol. **11**, 677 (2016).
[24] M. Pelliccione, A. Jenkins, P. Ovartchaiyapong, C. Reetz, E. Emmanouilidou, N. Ni, and A. C. Bleszynski Jayich, Nat. Nanotechnol. **11**, 700 (2016).
[25] F. Shi, Q. Zhang, P. Wang, H. Sun, J. Wang, X. Rong, M. Chen, C. Ju, F. Reinhard, H. Chen, J. Wrachtrup, J. Wang, and J. Du, Science **347**, 1135 (2015).
[26] T. Staudacher, F. Shi, S. Pezzagna, J. Meijer, J. Du, C. A. Meriles, F. Reinhard, and J. Wrachtrup, Science **339**, 561 (2013).
[27] I. Lovchinsky, A. O. Sushkov, E. Urbach, N. P. de Leon, S. Choi, K. De Greve, R. Evans, R. Gertner, E. Bersin, C. Müller, L. McGuinness, F. Jelezko, R. L. Walsworth, H. Park, and M. D. Lukin, Science **351**, 836 (2016).
[28] G. Kucsko, P. C. Maurer, N. Y. Yao, M. Kubo, H. J. Noh, P. K. Lo, H. Park, and M. D. Lukin, Nature (London) **500**, 54 (2013).
[29] P. Neumann, I. Jakobi, F. Dolde, C. Burk, R. Reuter, G. Waldherr, J. Honert, T. Wolf, A. Brunner, J. H. Shim, D. Suter, H. Sumiya, J. Isoya, and J. Wrachtrup, Nano Lett. **13**, 2738 (2013).
[30] A. Ariyaratne, D. Bluvstein, B. A. Myers, and A. C. B. Jayich, Nat. Commun. **9**, 2406 (2018).
[31] A. Faraon, P. E. Barclay, C. Santori, K.-M. C. Fu, and R. G. Beausoleil, Nat. Photonics **5**, 301 (2011).
[32] D. Lee, K. W. Lee, J. V. Cady, P. Ovartchaiyapong, and A. C. B. Jayich, J. Opt. **19**, 033001 (2017).
[33] J. Cai, A. Retzker, F. Jelezko, and M. B. Plenio, Nat. Phys. **9**, 168 (2013).
[34] T. Gaebel, M. Domhan, C. Wittmann, I. Popa, F. Jelezko, J. Rabeau, A. Greentree, S. Prawer, E. Trajkov, P. Hemmer, and J. Wrachtrup, Appl. Phys. B **82**, 243 (2006).
[35] K. Iakoubovskii, G. J. Adriaenssens, and M. Nesladek, J. Phys. Condens. Matter **12**, 189 (2000).
[36] N. Manson and J. Harrison, Diam. Relat. Mater. **14**, 1705 (2005).
[37] M. V. Hauf, B. Grotz, B. Naydenov, M. Dankerl, S. Pezzagna, J. Meijer, F. Jelezko, J. Wrachtrup, M. Stutzmann, F. Reinhard, and J. A. Garrido, Phys. Rev. B **83**, 081304 (2011).
[38] L. Rondin, G. Dantelle, A. Slablab, F. Grosshans, F. Treussart, P. Bergonzo, S. Perruchas, T. Gacoin, M. Chaigneau, H. C. Chang, V. Jacques, and J. F. Roch, Phys. Rev. B **82**, 115449 (2010).
[39] K.-M. C. Fu, C. Santori, P. E. Barclay, and R. G. Beausoleil, Appl. Phys. Lett. **96**, 121907 (2010).
[40] J. M. Taylor, P. Cappellaro, L. Childress, L. Jiang, D. Budker, P. R. Hemmer, A. Yacoby, R. Walsworth, and M. D. Lukin, Nat. Phys. **4**, 810 (2008).
[41] D. Rugar, H. J. Mamin, M. H. Sherwood, M. Kim, C. T. Rettner, K. Ohno, and D. D. Awschalom, Nat. Nanotechnol. **10**, 120 (2015).
[42] N. Aslam, G. Waldherr, P. Neumann, F. Jelezko, and J. Wrachtrup, New J. Phys. **15**, 013064 (2013).
[43] X.-D. Chen, C.-L. Zou, F.-W. Sun, and G.-C. Guo, Appl. Phys. Lett. **103**, 013112 (2013).
[44] Y. Doi, T. Fukui, H. Kato, T. Makino, S. Yamasaki, T. Tashima, H. Morishita, S. Miwa, F. Jelezko, Y. Suzuki, and N. Mizuochi, Phys. Rev. B **93**, 081203 (2016).
[45] Y. Doi, T. Makino, H. Kato, D. Takeuchi, M. Ogura, H. Okushi, H. Morishita, T. Tashima, S. Miwa, S. Yamasaki, P. Neumann, J. Wrachtrup, Y. Suzuki, and N. Mizuochi, Phys. Rev. X **4**, 011057 (2014).
[46] A. N. Newell, D. A. Dowdell, and D. H. Santamore, J. Appl. Phys. **120**, 185104 (2016).
[47] R. Giri, F. Gorrini, C. Dorigoni, C. E. Avalos, M. Cazzanelli, S. Tambalo, and A. Bifone, Phys. Rev. B **98**, 045401 (2018).
[48] J. Choi, S. Choi, G. Kucsko, P. C. Maurer, B. J. Shields, H. Sumiya, S. Onoda, J. Isoya, E. Demler, F. Jelezko, N. Y. Yao, and M. D. Lukin, Phys. Rev. Lett. **118**, 093601 (2017).
[49] S. Dhomkar, H. Jayakumar, P. R. Zangara, and C. A. Meriles, Nano Lett. **18**, 4046 (2018).
[50] S. Dhomkar, P. R. Zangara, J. Henshaw, and C. A. Meriles, Phys. Rev. Lett. **120**, 117401 (2018).
[51] S. Dhomkar, J. Henshaw, H. Jayakumar, and C. A. Meriles, Sci. Adv. **2**, e1600911 (2016).
[52] H. Jayakumar, J. Henshaw, S. Dhomkar, D. Pagliero, A. Laraoui, N. B. Manson, R. Albu, M. W. Doherty, and C. A. Meriles, Nat. Commun. **7**, 12660 (2016).
[53] See Supplemental Material at http://link.aps.org/supplemental/10.1103/PhysRevLett.122.076101 for supporting data, analysis, and methodological details, which includes Refs. [54–56].
[54] J. R. Rabeau, P. Reichart, G. Tamanyan, D. N. Jamieson, S. Prawer, F. Jelezko, T. Gaebel, I. Popa, M. Domhan, and J. Wrachtrup, Appl. Phys. Lett. **88**, 023113 (2006).
[55] D. M. Toyli, C. D. Weis, G. D. Fuchs, T. Schenkel, and D. D. Awschalom, Nano Lett. **10**, 3168 (2010).
[56] R. Farrer, Solid State Communications **7**, 685 (1969).
[57] L. M. Pham, S. J. DeVience, F. Casola, I. Lovchinsky, A. O. Sushkov, E. Bersin, J. Lee, E. Urbach, P. Cappellaro, H. Park, A. Yacoby, M. Lukin, and R. L. Walsworth, Phys. Rev. B **93**, 045425 (2016).
[58] A. Ajoy, Y.-X. Liu, K. Saha, L. Marseglia, J.-C. Jaskula, U. Bissbort, and P. Cappellaro, Proc. Natl. Acad. Sci. U.S.A. **114**, 2149 (2017).
[59] L. Hacquebard and L. Childress, Phys. Rev. A **97**, 063408 (2018).
[60] H. J. Mamin, M. Kim, M. H. Sherwood, C. T. Rettner, K. Ohno, D. D. Awschalom, and D. Rugar, Science **339**, 557 (2013).
[61] M. Loretz, J. M. Boss, T. Rosskopf, H. J. Mamin, D. Rugar, and C. L. Degen, Phys. Rev. X **5**, 021009 (2015).

[62] P. Deák, B. Aradi, M. Kaviani, T. Frauenheim, and A. Gali, Phys. Rev. B **89**, 075203 (2014).

[63] A. Stacey, N. Dontschuk, J.-P. Chou, D. A. Broadway, A. Schenk, M. J. Sear, J.-P. Tetienne, A. Hoffman, S. Prawer, C. I. Pakes, A. Tadich, N. P. de Leon, A. Gali, and L. C. L. Hollenberg, Adv. Mater. Interfaces, DOI: 10.1002/admi.201801449.

[64] B. A. Myers, A. Ariyaratne, and A. C. Bleszynski Jayich, Phys. Rev. Lett. **118**, 197201 (2017).

[65] J.-P. Chou, Z. Bodrog, and A. Gali, Phys. Rev. Lett. **120**, 136401 (2018).

[66] F. Dolde, M. W. Doherty, J. Michl, I. Jakobi, B. Naydenov, S. Pezzagna, J. Meijer, P. Neumann, F. Jelezko, N. B. Manson, and J. Wrachtrup, Phys. Rev. Lett. **112**, 097603 (2014).

[67] T. Mittiga, S. Hsieh, C. Zu, B. Kobrin, F. Machado, P. Bhattacharyya, N. Rui, A. Jarmola, S. Choi, D. Budker, and N. Y. Yao, Phys. Rev. Lett. **121**, 246402 (2018).